J Supercond Nov Magn (2016) 29:1377–1386
DOI 10.1007/s10948-016-3422-5

ORIGINAL PAPER

# Magnetic Characterization of Nanocrystalline Co-B-Si-Fe-Mo Alloys

**Mohammad Reza Jafari Jezeh[1] · Majid Tavoosi[1] · Ali Ghasemi[1] · Reza Farshadnia[2]**

Received: 28 November 2015 / Accepted: 20 January 2016 / Published online: 5 February 2016


**Abstract** Fabrication of nanocrystalline Co-B-Si-Fe-Mo magnetic alloys by means of mechanical alloying was the goal of this study. In this regard, different powder mixtures containing $Co_{70}B_{30-x}Si_x$ ($x = 10, 15, 20$) and $Co_{70}B_{20}Si_5Fe_{5-x}Mo_x$ ($x = 0, 2.5, 5$) (at.%) were mechanically milled in a planetary ball mill for different periods of time. The produced samples were characterized using X-ray diffraction (XRD), scanning electron microscopy (SEM), and vibrating sample magnetometer (VSM). The produced alloys exhibit magnetic properties with the saturation of magnetization and coercivity in the range of 30–260 Oe and 100–180 emu/g, respectively. The highest saturation of magnetization and the lowest coercivity appear in alloys with higher B content. Moreover, Fe element has a suitable effect and Mo element has a destructive effect on soft magnetic properties of $Co_{70}B_{20}Si_5Fe_{5-x}Mo_x$ alloys.

**Keywords** Co-based · Nanocrystalline · Mechanical alloying · Soft magnetic

## 1 Introduction

Nanocrystalline materials are a class of materials with grain sizes smaller than 100 nm, which are synthesized by a variety of techniques such as severe plastic deformation (SPD), mechanical alloying (MA), inert gas condensation, and electrodeposition processes [1, 2]. Interest in these materials is due to their high mechanical, physical, and chemical properties [3]. Since these materials are characterized by low crystalline size and their high volume fraction of grain boundaries may comprise as much as 10−50 % of the total crystal volume, their magnetic behavior may be quite different from those of their coarse grain counterparts. In fact, the nanocrystaline materials display a very low magnetic anisotropy. This is caused by the fact that the originated grains are significantly smaller than the correlation length of the ferromagnetic exchange interactions [4].

Co-based soft magnetic materials were commercialized due to their very high magnetic permeability and low coercivity. There is a possibility of obtaining a low magnetostriction in both the amorphous and crystalline phases, which is highly desirable from the stand point of technical applications [5–7]. In fact, these materials are ideal choices as cores of inductive components used up to frequencies of 1 MHz in digital telecommunication circuits. Boron and silicon are common alloying elements in Co-based alloys. The addition of these metalloid elements to Co-based alloys improves their ability to form amorphous as well as nanocrystalline phases. However, B and Si elements can dilute the magnetic moments of Co-B-Si alloys. The soft magnetic properties of these alloys can be affected by some additive elements (substituted for the metalloids), which change the configuration of magnetic moments and can improve their magnetic properties [8].

Although there are a lot of studies about the formation and characterization of Co-based alloys [9–13], the exact effects of B, Si, Fe, and Mo elements on the structural and magnetic properties of these alloys have not been properly

✉ Majid Tavoosi
ma.tavoosi@gmail.com

[1] Department of Materials Engineering, Malek-Ashtar University of Technology (MUT), Shahin-Shahr, Isfahan, Iran

[2] Department of Materials Science, Iran University of Science and Technology (IUST), Tehran, Iran

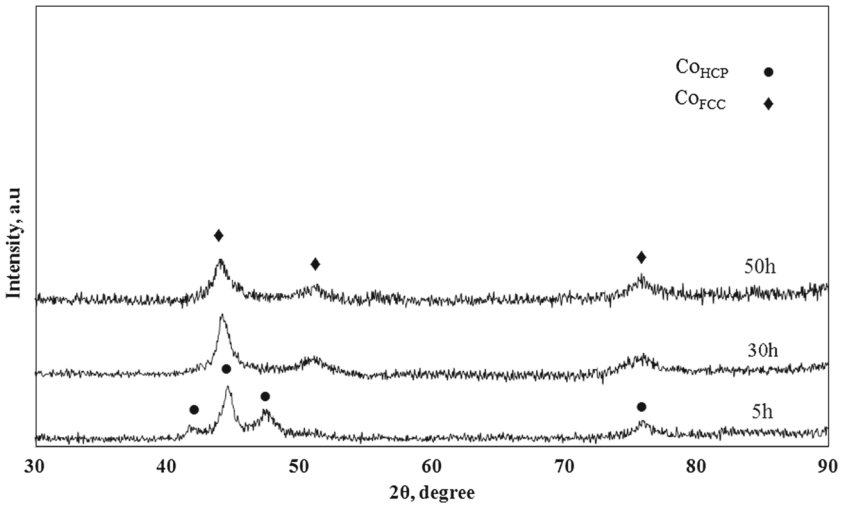


**Fig. 1** The XRD patterns of $Co_{70}B_{10}Si_{20}$ powder mixture milled for different periods of time

investigated. So, determination of the effect of B, Si, Fe, and Mo elements on the magnetic properties of Co-based alloys is the goal of this study.

## 2 Experimental Procedures

Co (Merck, 99.8 % purity), B (Merck, 99.8 % purity), Si (Merck, 99.8 % purity), Fe (Merck, 99.8 % purity), and Mo (Merck, 99.8 % purity) were used as raw materials. The elemental powders with the composition of $Co_{70}B_{30-x}Si_x$ ($x = 10, 15, 20$) and $Co_{70}B_{20}Si_5Fe_{5-x}Mo_x$ ($x = 0, 2.5, 5$) (at.%) were mechanically milled in a planetary ball mill in an argon atmosphere (the rotation speed of 800 rpm and the ball to powder ratio of 20:1). Using a diffractometer with Cu Ka radiation ($\lambda = 0.15406$ nm; 40 kV; Philips PW3710), X-ray diffraction (XRD) technique was used to follow the structural changes of the specimens (step size, 0.05°; time per step, 1 s). The average crystallite sizes of the produced samples were estimated by analyzing broadening of XRD peaks using scherrer formula [14]. Morphological characterization of the samples was carried out by scanning electron microscopy (VEGA-TESCAN-XMU) at an accelerating voltage of 20 kV. Magnetic properties (saturation magnetization and approximate coercivity) of produced samples were also measured using a vibrating scanning magnetometer (VSM) under an applied field up to 15 kOe.

## 3 Results and Discussion

### 3.1 $Co_{70}B_{30-x}Si_x$ ($x = 10, 15, 20$) Alloys

#### *3.1.1 Structural Characterization*

The XRD patterns of $Co_{70}B_{10}Si_{20}$ powder mixture, after various MA processing periods, are shown in Fig. 1. In the early stage of the MA process, only the broadening of the

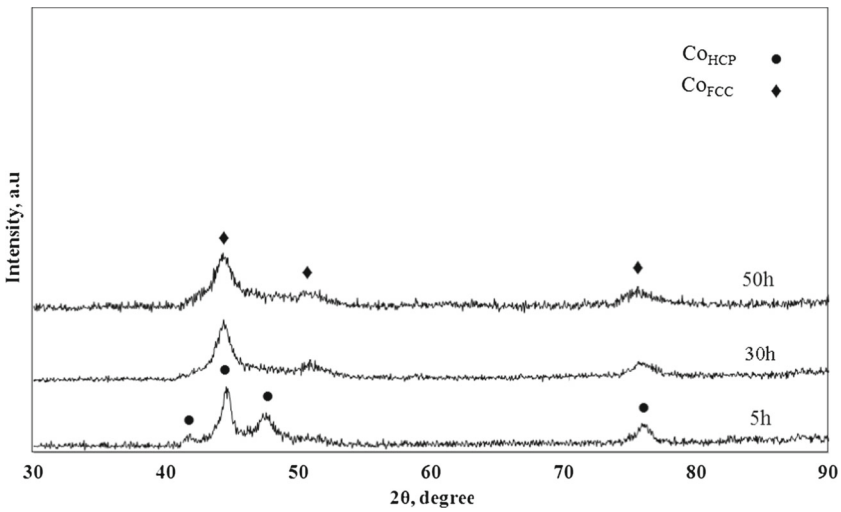


**Fig. 2** The XRD patterns of $Co_{70}B_{15}Si_{15}$ powder mixture milled for different periods of time

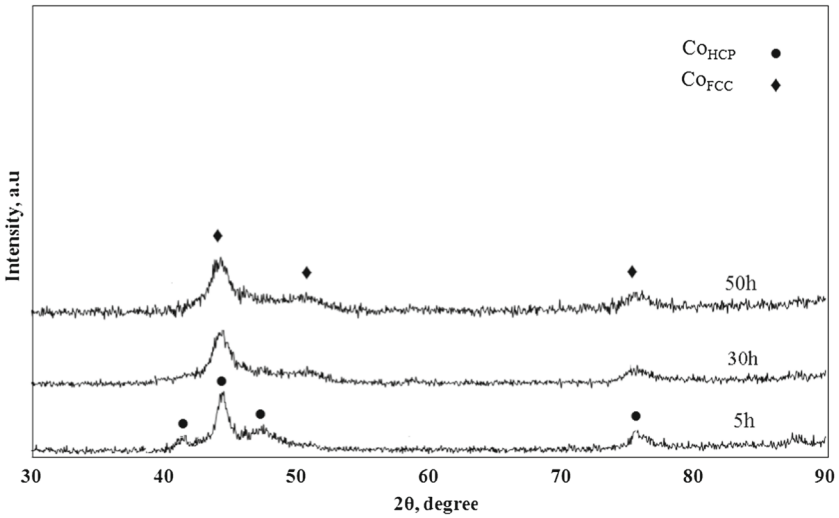


**Fig. 3** The XRD patterns of $Co_{70}B_{20}Si_{10}$ powder mixture milled for different periods of time

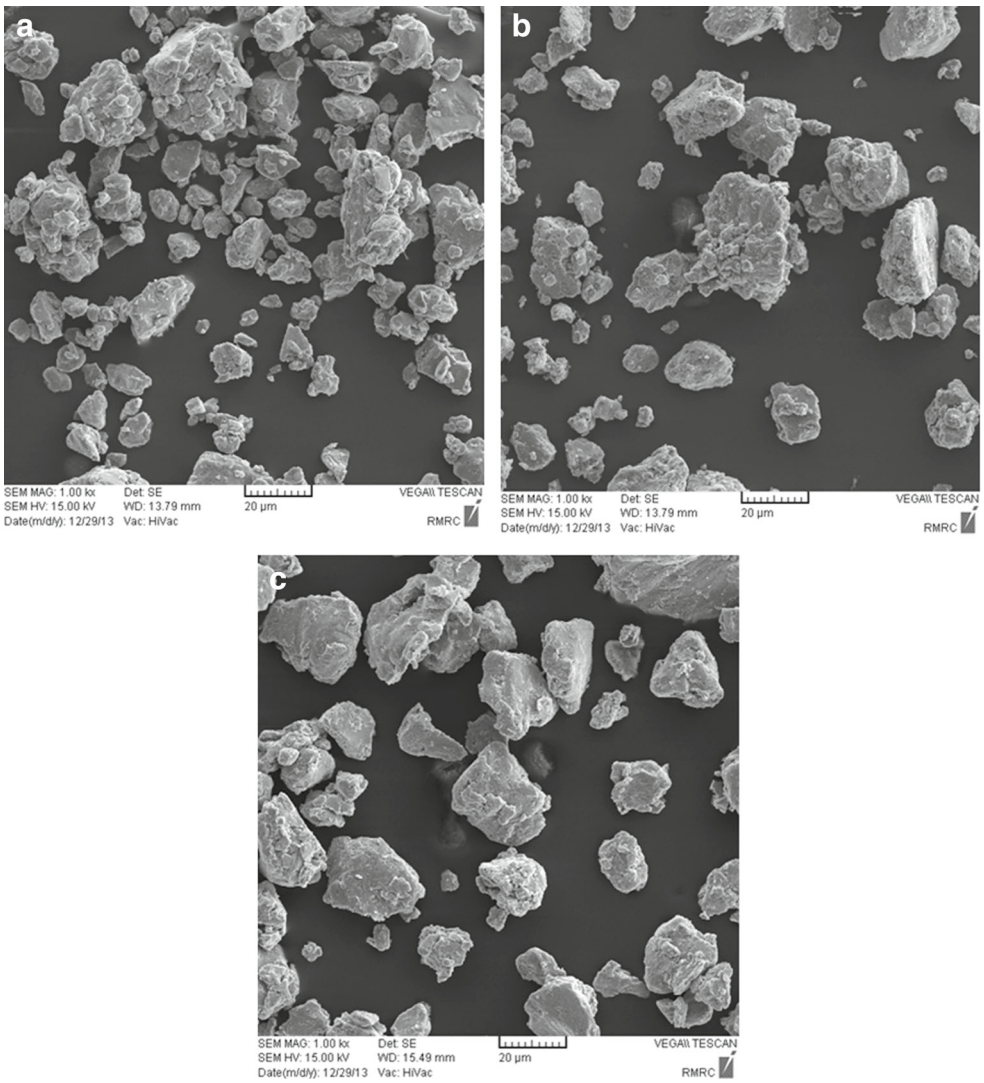


**Fig. 4** The SEM micrographs of **a** $Co_{70}B_{10}Si_{20}$, **b** $Co_{70}B_{15}Si_{15}$, and **c** $Co_{70}B_{20}Si_{10}$ powder mixture alloys after 50 h of milling time

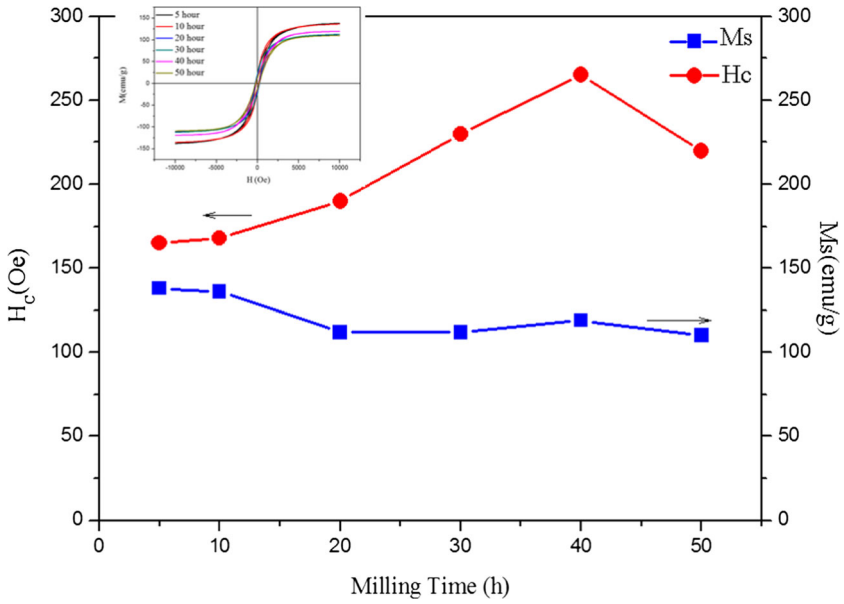


**Fig. 5** The change in coercivity and saturation of magnetization of $Co_{70}B_{10}Si_{20}$ as a function of milling time

initial element peaks accompanied by remarkable decreases in their intensities occurred as a result of the crystalline sizes refinement and lattice strains increments. Increasing milling time to 5 h led to the disappearance of the B and Si peaks, while the Co peaks shifted to lower angles. This can be due to the dissolution of B and Si in Co lattice and formation of $Co_{HCP}$ solid solution. In fact, increasing the density of crystalline defects such as phase and grain boundaries, dislocations, and vacancies is the main reason for the formation of $Co_{HCP}$ solid solution during mechanical alloying [15].

By increasing the milling time, two peaks corresponding to $Co_{FCC}$ phase (high-temperature allotropy of cobalt) appeared in the XRD patterns. The observed $Co_{FCC}$ peaks demonstrate the formation of this metastable phase from the mechanically milled $Co_{HCP}$ solid solution. These results are in agreement with those obtained by Bolarin-Miro and Bednarcik et al. [16, 17]. These researchers showed that by milling the $Co_{HCP}$ solid solution, the amount of stacking faults, especially for twin type, increases and the HCP unit cell of cobalt is distorted. In fact, the distortion of $Co_{HCP}$ structure by increasing the stacking faults (rather than the local temperature rise and reduction in the crystallite sizes) is the main mechanism governing the HCP to FCC transformation at room temperature [18].

Analysis of the XRD patterns reveals that after 30 h of milling, gradual grain refinement is the only considerable change that occurs in the powder mixture, and no detectable reaction takes place. Moreover, the average crystallite sizes

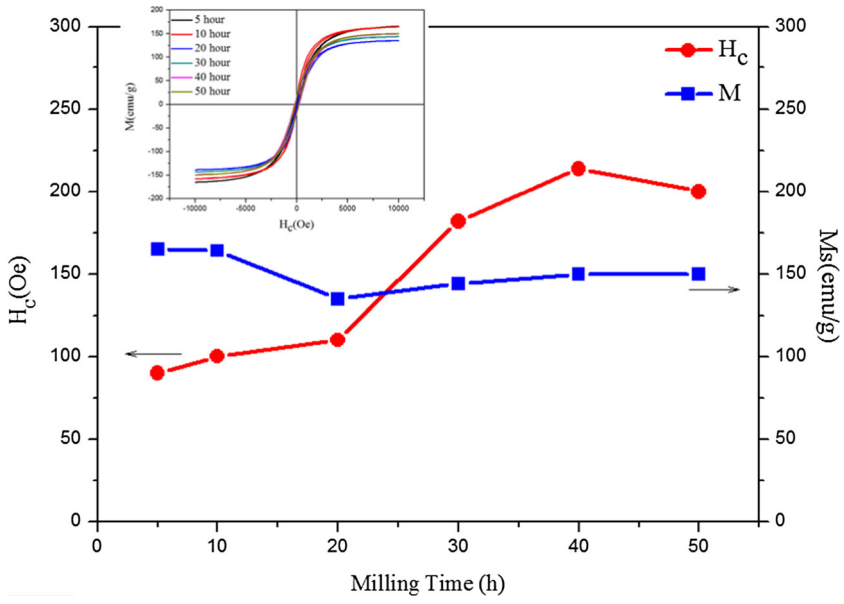


**Fig. 6** The change in coercivity and saturation of magnetization of $Co_{70}B_{15}Si_{15}$ as a function of milling time

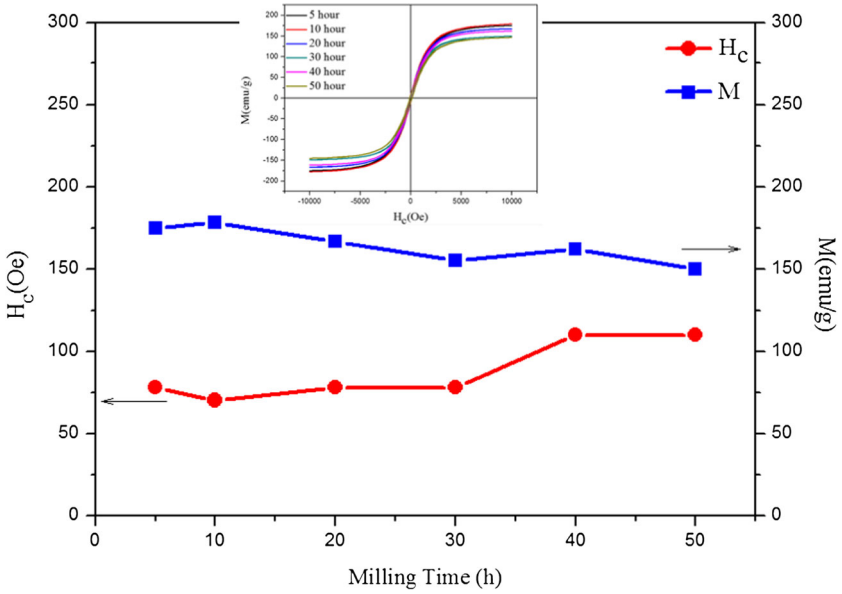


**Fig. 7** The change in coercivity and saturation of magnetization of $Co_{70}B_{20}Si_{10}$ as a function of milling time

of formed $Co_{HCP}$ and $Co_{FCC}$ phases after 50 h of milling were estimated to be about 10 nm.

Similar to $Co_{70}B_{10}Si_{20}$, the XRD patterns of the $Co_{70}B_{15}Si_{15}$ and $Co_{70}B_{20}Si_{10}$ powder blends subjected to the MA process are also presented in Figs. 2 and 3, respectively. According to these figures, the structural changes during mechanical alloying in these two alloying systems are very similar to $Co_{70}B_{10}Si_{20}$ system, and these changes (until 50 h) can be written as follows:

$$\text{Powder mixture} \rightarrow Co_{HCP} \rightarrow Co_{HCP} + Co_{FCC}.$$

The scanning electron microscopy (SEM) micrographs of milled powders in different Co-B-Si alloying systems after 50 h of milling are shown in Fig. 4. It was found that there is no appreciable different between the particle size and the morphology of produced alloys in different alloying systems.

### *3.1.2 Magnetic Characterization*

Changes in the saturation of magnetization and coercivity of $Co_{70}B_{10}Si_{20}$ powder mixture as a function of milling times (extracted from the hysteresis loops) are presented in Fig. 5. As seen, the coercivity and saturation of magnetization of milled samples after 5 h of milling are about 165 Oe and 138 emu/g, respectively. By progression of the milling time, the coercivity increases and reaches a constant value of about 260 Oe. This change may be attributed to the decrease in crystallite sizes, increase in the internal strain, and the precipitation of $Co_{FCC}$ phase in matrix during milling process. In contrast to coercivity, by milling the $Co_{70}B_{10}Si_{20}$

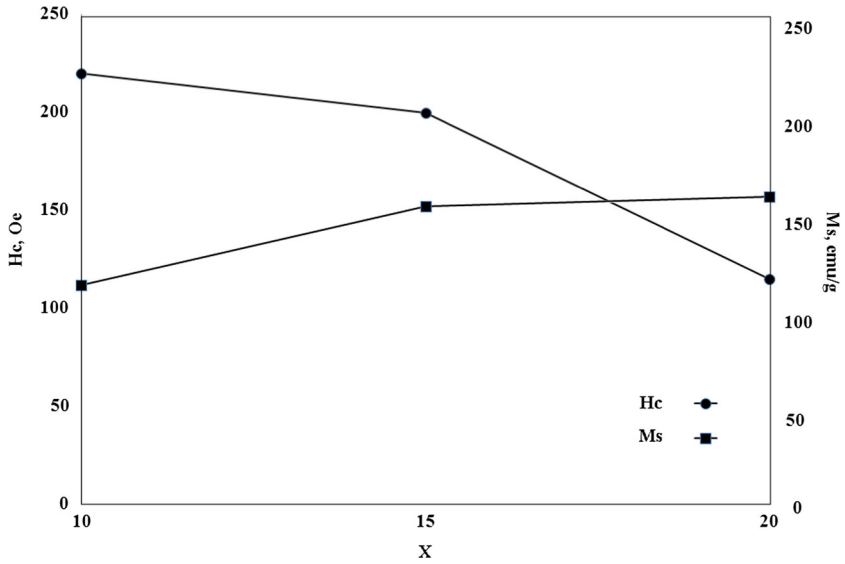


**Fig. 8** The coercivity and saturation of magnetization of produced $Co_{70}B_{30-x}Si_x$ ($x = 10, 15, 20$) alloys after 50 h of milling

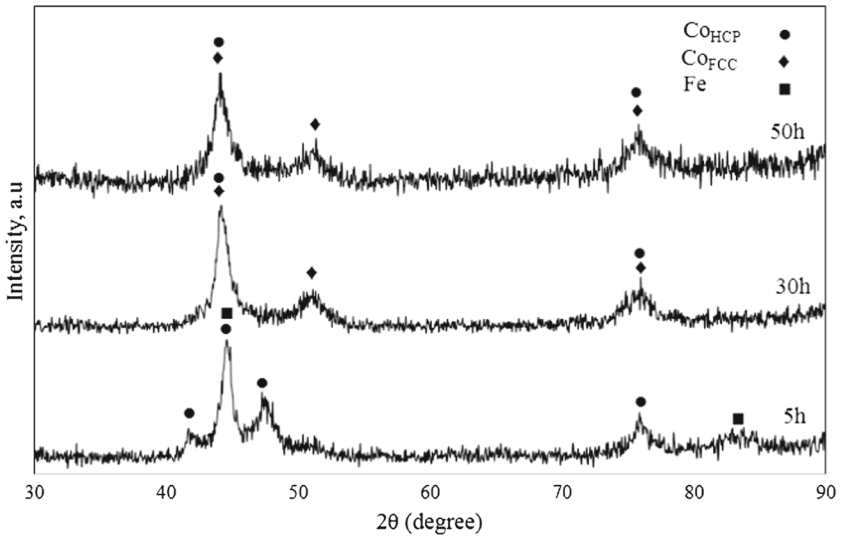


**Fig. 9** The XRD patterns of $Co_{70}B_{20}Si_5Fe_5$ powder mixture milled for different periods of time

powder mixture, the saturation of magnetization values remains constant.

Changes in the saturation of magnetization and coercivity of $Co_{70}B_{15}Si_{15}$ and $Co_{70}B_{20}Si_{10}$ powder mixture as a function of milling times are also presented in Figs. 6 and 7, respectively. According to these figures, the changes in magnetic properties of $Co_{70}B_{15}Si_{15}$ and $Co_{70}B_{20}Si_{10}$ powder mixtures during mechanical alloying are very similar to $Co_{70}B_{10}Si_{20}$ powder mixture. In fact, this behavior can be related to the same structural changes which accrued during mechanical alloying in these three systems.

The coercivity and saturation of magnetization of produced $Co_{70}B_{30-x}Si_x$ ($x = 10, 15, 20$) alloys after 50 h of milling are presented in Fig. 8. As seen, by replacing the Si with B element, the saturation of magnetization increases from 110 to 150 emu/g and the coercivity decreases from 220 to 110 Oe. In fact, structural and morphological characterizations of these three alloys (by attention to XRD and SEM results) are the same, and the difference in magnetic properties can only be due to the effect of B and Si in composition. This effect may be attributed to several factors as explained bellow:

1. Silicon is a diamagnetic element. Increasing the amount of this element in Co-based alloys can decrease the soft magnetic properties.
2. Silicon has larger atomic size than boron. Increasing the Si content can increase the stress magnetic anisotropy of the sample and decrease the soft magnetic properties [19].

### 3.2 $Co_{70}B_{20}Si_5Fe_{5-x}Mo_x$ ($x = 0, 2.5, 5$) Alloys

#### *3.2.1 Structural Characterizations*

By paying attention to the previous section, the soft magnetic properties of $Co_{70}B_{20}Si_{10}$ alloy are better than alloys

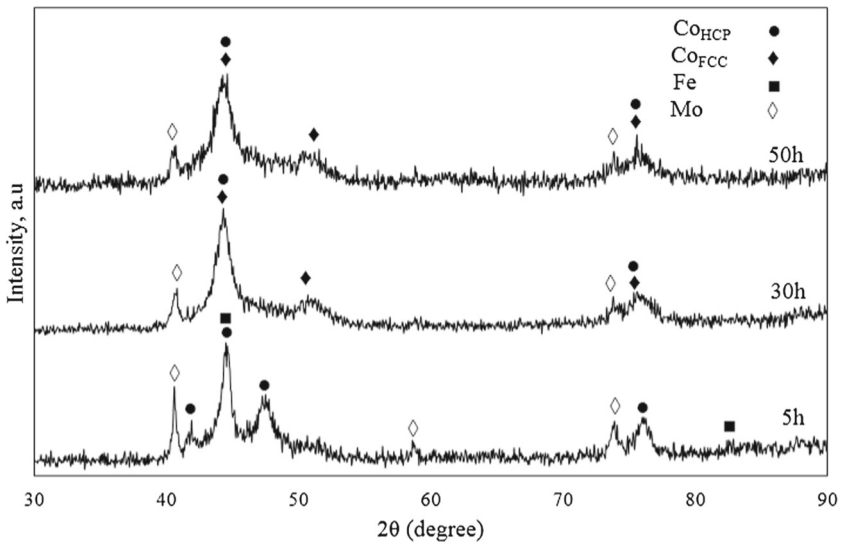


**Fig. 10** The XRD patterns of $Co_{70}B_{20}Si_5Fe_{2.5}Mo_{2.5}$ powder mixture milled for different periods of time

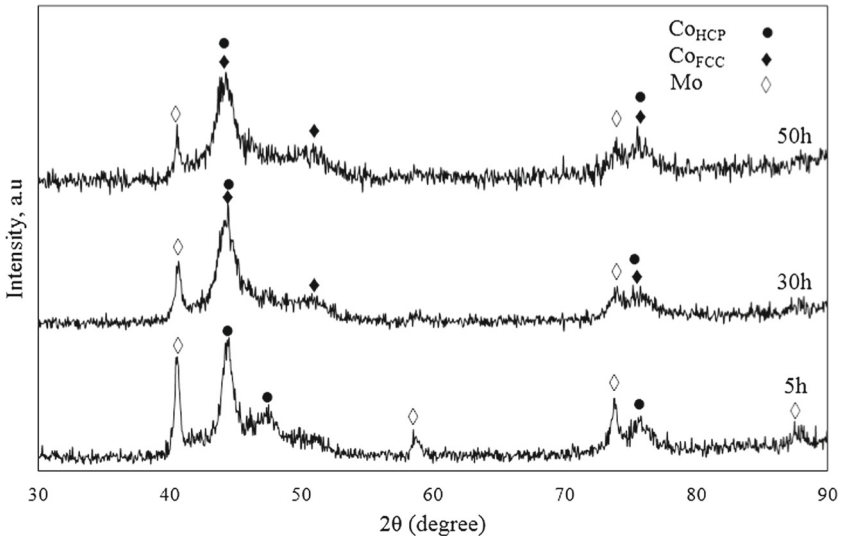


**Fig. 11** The XRD patterns of $Co_{70}B_{20}Si_5Mo_5$ powder mixture milled for different periods of time

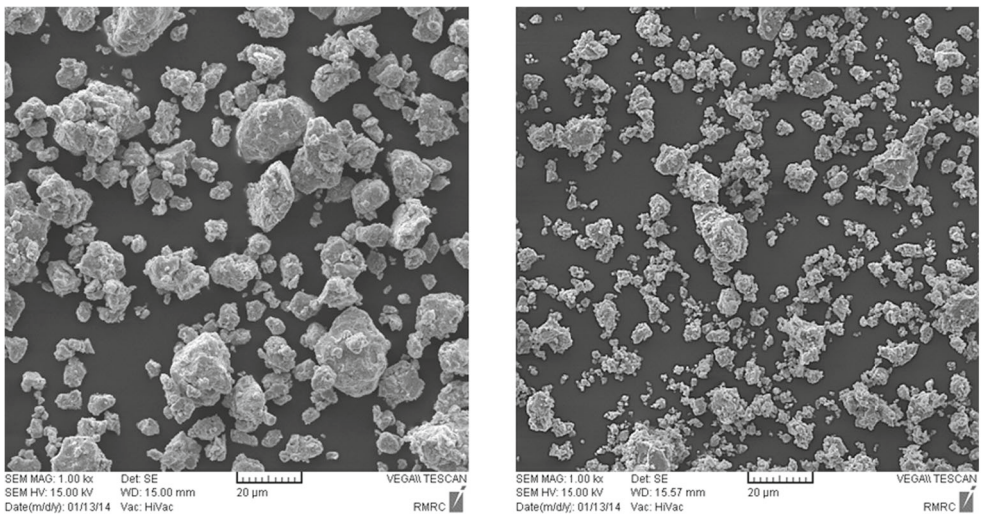


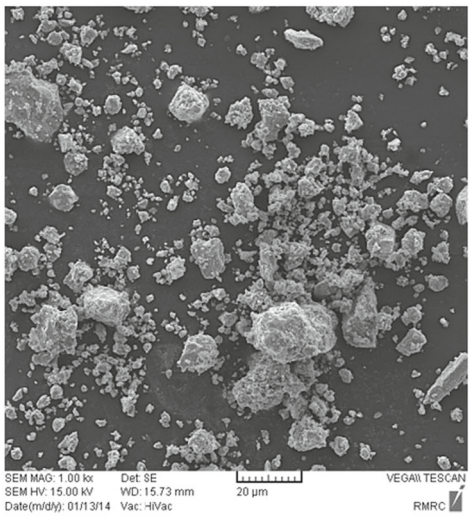


**Fig. 12** The SEM micrographs of **a** $Co_{70}B_{20}Si_5Fe_5$, **b** $Co_{70}B_{20}Si_5Fe_{2.5}Mo_{2.5}$, and **c** $Co_{70}B_{20}Si_5Mo_5$ alloys after 50 h of milling time

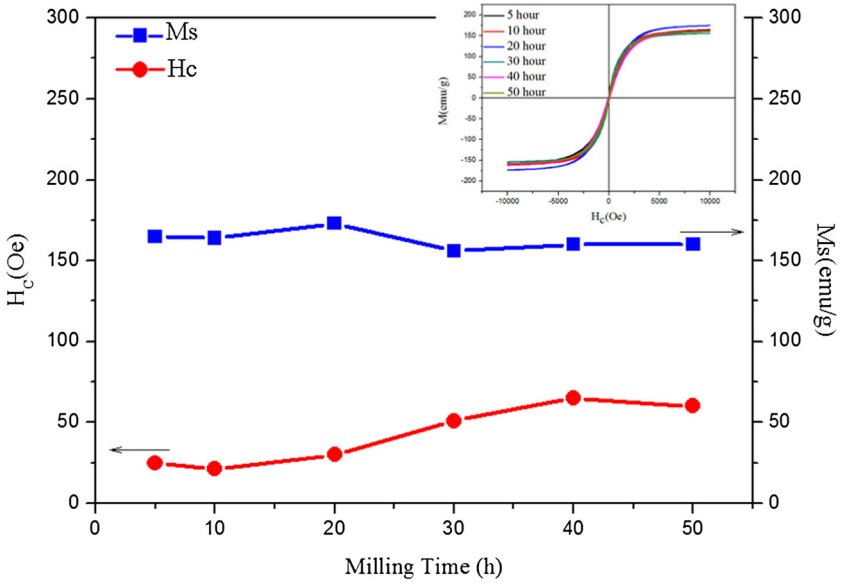


**Fig. 13** The change in coercivity and saturation of magnetization of $Co_{70}B_{20}Si_5Fe_5$ powder mixture as a function of milling time

with higher silicon content. In this section, the effect of Mo and Fe elements substituted for Si content on magnetic properties of $Co_{70}B_{20}Si_5Fe_{5-x}Mo_x$ ($x = 0, 2.5, 5$) alloy has been investigated.

The XRD patterns of $Co_{70}B_{20}Si_5Fe_5$, $Co_{70}B_{20}Si_5Fe_{2.5}Mo_{2.5}$, and $Co_{70}B_{20}Si_5Mo_5$ powder mixtures after different milling times are presented in Figs. 9, 10 and 11. By paying attention to these XRD patterns, several points can be concluded as the following:

1. The structural changes in $Co_{70}B_{20}Si_5Fe_5$ alloy during mechanical alloying are similar to Co-B-Si alloys and can be written as follows: Powder mixture→ $Co_{HCP}$ → $Co_{HCP}$+ $Co_{FCC}$.
2. Besides the $Co_{70}B_{20}Si_5Fe_5$ powder blended, the XRD patterns of the $Co_{70}B_{20}Si_5Mo_5$ and $Co_{70}B_{20}Si_5Fe_{2.5}Mo_{2.5}$ powder mixtures after 50 h of milling are contains of Mo peaks. These results illustrated that during milling up to 50 h, Mo atoms could not dissolve in Co lattice. In fact, the lattice mismatch between Co and Mo is very high and the dissolution of this element in Co lattice needs higher milling times [15]. Consequently, the final structures of these two alloying systems after mechanical alloying are a combination of $Co_{HCP}$, $Co_{FCC}$, and residual Mo.
3. The average crystalline sizes of the Co phases in different alloying systems, estimated with scherrer formula, were about 10 nm. The SEM micrographs of

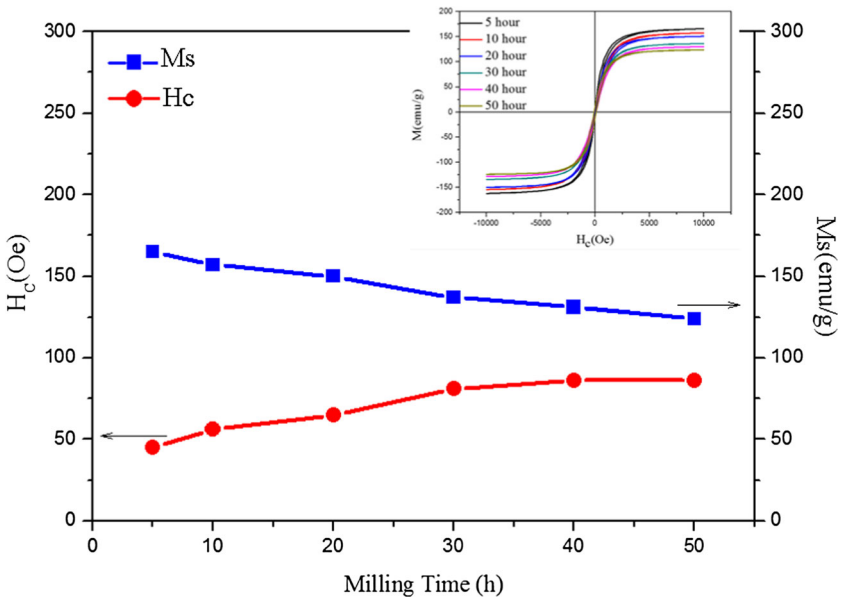


**Fig. 14** The change in coercivity and saturation of magnetization of $Co_{70}B_{20}Si_5Fe_{2.5}Mo_{2.5}$ powder mixture as a function of milling time

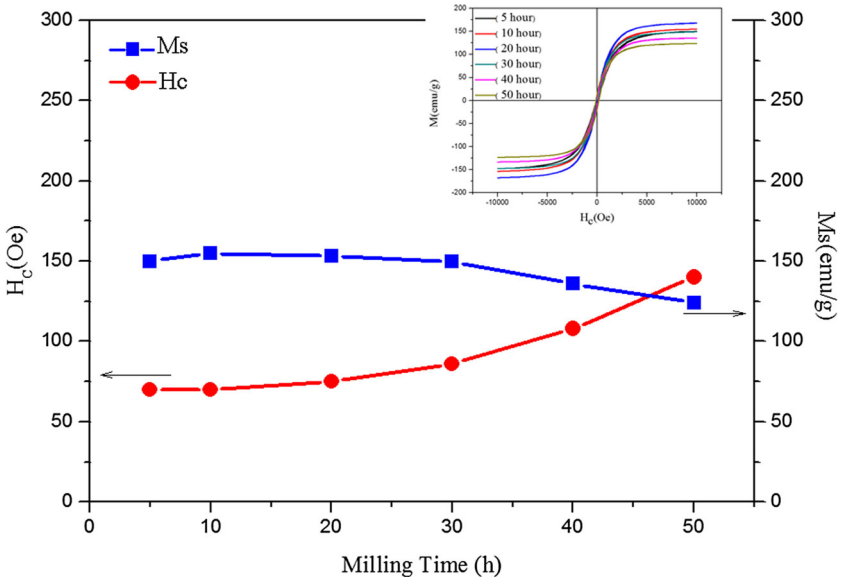


**Fig. 15** The change in coercivity and saturation of magnetization of $Co_{70}B_{20}Si_5Mo_5$ powder mixture as a function of milling time

$Co_{70}B_{20}Si_5Fe_{5-x}Mo_x$ ($x = 0, 2.5, 5$) milled powders after 50 h of milling are also presented in Fig. 12. According to these results, the average crystallte size, particle size, and morphology of different samples are the same and independent of the chemical composition.

### *3.2.2 Magnetic Characterizations*

The change in saturation of magnetization and the coercivity of $Co_{70}B_{20}Si_5Fe_5$, $Co_{70}B_{20}Si_5Fe_{2.5}Mo_{2.5}$, and $Co_{70}B_{20}Si_5Mo_5$ powder mixtures as a function of milling time are presented in Figs. 13, 14 and 15, respectively. According to these figures, high energy ball milling in these alloying systems cause a significant increase in the coercivity and slight changes in saturation of magnetization. Just as above, these changes may also be attributed to the decrease in crystallite sizes and increase in the internal strain and the precipitation of $Co_{FCC}$ phase in matrix during milling process.

The coercivity and saturation of magnetization of produced $Co_{70}B_{20}Si_5Fe_{5-x}Mo_x$ ($x = 0, 2.5, 5$) powders after 50 h of milling are presented in Fig. 16. As seen, the magnetic properties of the produced alloys strongly depend on their composition. The alloys with higher content of Fe exhibit the highest saturation of magnetization and the lowest coercivity. For example, the coercivity and the saturation of magnetization of nanocrystalline $Co_{70}B_{20}Si_5Fe_5$ alloy were about 60 Oe and 155 emu/g, whereas these values for nanocrystalline $Co_{70}B_{20}Si_5Mo_5$ alloy were 150 Oe and 124 emu/g, respectively. This effect may be attributed to the following:

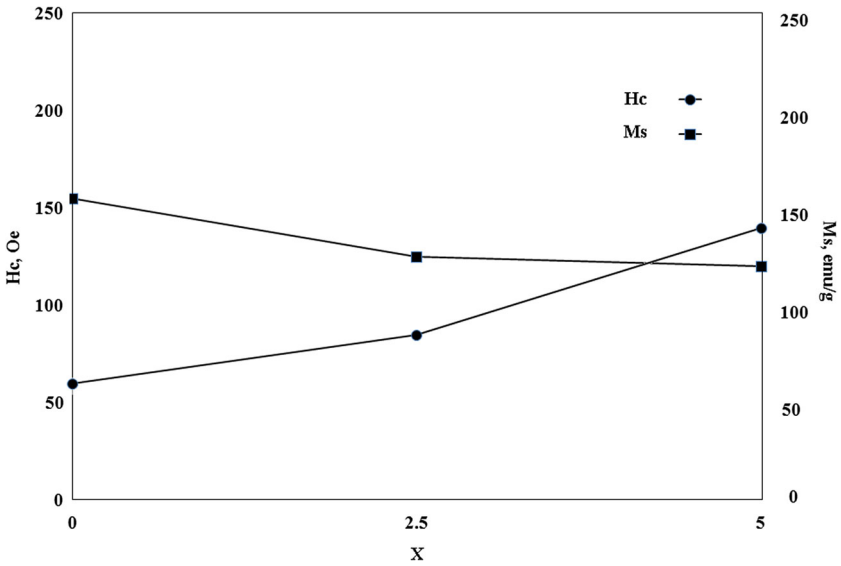


**Fig. 16** The coercivity and saturation of magnetization of produced $Co_{70}B_{20}Si_5Fe_{5-x}Mo_x$ ($x = 0, 2.5, 5$) alloys after 50 h of milling

1. Suitable soft magnetic properties of alloys are directly proportional to their magnetostriction coefficient, and the alloys with less magnetostriction coefficient show better soft magnetic properties. In fact, the $Co_{70}B_{20}Si_5Fe_5$ alloy has less magnetostriction than the $Co_{70}B_{20}Si_5Fe_{2.5}Mo_{2.5}$ and $Co_{70}B_{20}Si_5Mo_5$ alloys [20].
2. The exchange interaction between Mo and Co atoms is an anti-ferromagnetic type [20]. Therefore, addition of Mo atoms to alloy introduces anti-ferromagnetic moments into the alloys and cancels out some ferromagnetic moments of Co leading to the reduction in the ferromagnetic moments.
3. Cobalt has a very strong ferromagnetic exchange coupled with Fe, and addition of Fe could lead to the alignment of the Co moments, thereby increasing the atomic magnetic moment of individual Co atoms [20].

## 4 Conclusion

In the present paper, fabrication and magnetic characterization of nanocrystalline Co-based alloys by means of mechanical alloying have been investigated. The results showed that the structural changes during mechanical alloying in $Co_{70}B_{30-x}Si_x$ ($x = 10, 15, 20$) alloying system are the same (Powder mixture→ $Co_{HCP}$ solid solution→ $Co_{HCP}$+$Co_{FCC}$ solid solution) and the milling products are the combination of nanocrystalline $Co_{HCP}$ (10 nm) and $Co_{FCC}$ (10 nm) phases. The produced alloys exhibit soft magnetic properties with the saturation of magnetization and coercivity in the range of 30–260 Oe and 100–180 emu/g, respectively. The highest saturation of magnetization and the lowest coercivity in Co-B-Si system appear in the alloy with higher B content. The alloys with higher content of Fe in $Co_{70}B_{20}Si_5Fe_{5-x}Mo_x$ ($x = 0, 2.5, 5$) alloys exhibit the highest saturation of magnetization and the lowest coercivity. It was found that increase in the amount Fe and decrease in the amount of Mo enhances the soft magnetic properties of Co-based alloys.

## References


1. Whang, S.H.: Nanostructured Metals and Alloys, Processing, Microstructure, Mechanical Properties and Applications. Woodhead Publishing Limited, New York (2011)
2. Suryanarayana, C.: Mechanical Alloying and Milling. Taylor and Francis Group, New York (2004)
3. El-Eskandarany, M.S.: Mechanical Alloying for Fabrication of Advanced Engineering Materials. Noyes Publications, New York (2001)
4. Gehrmann, B.: Nickel–iron alloys with special soft magnetic properties for specific applications. J. Magn. Magn. Mater. **290-291**, 1419–142 (2005)
5. O'Handley, R.C.: Modern Magnetic Material Principle and Application. Wiley, New York (2000)
6. Dobrzanski, L.A., Nowosielski, R., Przyby, A., Konieczny, J.: Soft magnetic nanocomposite with powdered metallic ribbon based on cobalt and polymer matrix. J. Mat. Proc. Tech. **162-163**, 20–26 (2005)
7. Babilas, R., Nowosielski, R., Dercz, G., Stokłosa, Z., Głuchowski, W.: Influence of structure on soft magnetic properties of $Co_{70}Fe_5Si_{15}B_{10}$ metallic glass ribbons. Arch. Mat. Sci. Eng **54**, 37–44 (2012)
8. Voropaeva, L., Gurov, A., Stelmukh, V.: Medium range ordering and crystallization of Co-Si-B with Fe additions. J. Non-Crystalline Solids **192–193**, 153–156 (1995)
9. Wang, W., Ma, T., Yan, M.: Microstructure and magnetic properties of nanocrystalline Co-doped alloys prepared by melt spinning. J. All. Comp. **459**, 447–451 (2008)
10. Muhgalin, V.V., Dorofeev, G.A.: Nanocrystallization of the amorphous Co–B–Si alloys formed by melt spinning and mechanical alloying. Phys. Met. Metallogr. **112**, 596–602 (2011)
11. Sheverdyaeva, P.M., Prudnikov, V.N., Prov, N.S.: Effect of heat treatment on transport and magnetic properties of Co-based amorphous alloys. J. Non-Crystalline solids **353**, 869–871 (2007)
12. Dmitrieva, N.V., Lukshina, V.A., Volkova, E.G., Potapov, A.P., Filippov, B.N.: Fe and Co based nanocrystalline soft magnetic alloys modified with Hf, Mo, and Zr. Phys. Met. Metallogr. **114**, 138–144 (2013)
13. Skorvanek, I., Marcin, J., Turcanova, J.: Feco-based soft magnetic nanocrystalline alloys. Acta Electrotechnica et Informatica **10**, 14–18 (2010)
14. Cullity, B.D.: Elements of X-ray Diffraction. Addison-Wesley Publishing Company, London (1956)
15. Taghvaei, A.H., Stoica, M., Vaughan, G., Ghaffari, M., Maleksaeedi, S., Janghorban, K.: Microstructural characterization and amorphous phase formation in $Co_{40}Fe_{22}Ta_8B_{30}$ powders produced by mechanical alloying. J. All. Comp. **512**, 85–93 (2012)
16. Bolarin-Miró, A.M., Sánchez-De Jesús, F., Torres-villaseñor, G., Cortés-Escobedo, C.A., Betancourt-Cantera, J.A., Betancourt-Reyes, J.I.: Amorphization of Co-base alloy by mechanical alloying. J. Non-Crystalline Solids **357**, 1705–1709 (2011)
17. Bednarcik, J., Kovac, J.: Crystallization of CoFeSiB metallic glass induced by long-time ball milling. J. Non-Crystalline Solids **337**, 42–47 (2004)
18. Azzaza, S., Alleg, S., Suñol, J.: Phase transformation in the ball milled $Fe_{31}Co_{31}Nb_8B_{30}$ powders. Adv. Mat. Phy. Chem. **3**, 90–100 (2013)
19. Bahrami, A.H., Sharafi, S., Ahmadian, H.: The effect of Si addition on the microstructure and magnetic properties of permalloy prepared by mechanical alloying method. Adv. Powder Technol. **24**, 235–241 (2013)
20. Jiao, Z.B., Li, H.X., Gao, J.E., Wu, Y., Lu, Z.P.: Effects of alloying elements on glass formation, mechanical and soft-magnetic properties of Fe-based metallic glasses. Intermetallics **19**, 1502–1508 (2011)